RI 9247 REPORT OF INVESTIGATIONS/1989

RI 9247

LIBRARY
SPOKANE RESEARCH CENTER
RECEIVED

JUL 13 1989

U.S. BUREAU OF MINES
E 315 MONTGOMERY AVE.
SPOKANE, WA 99207

Effects of Abandoned Multiple Seam Workings on a Longwall in Virginia

By Gregory J. Chekan, Rudy J. Matetic,
and David L. Dwyer

BUREAU OF MINES

UNITED STATES DEPARTMENT OF THE INTERIOR

U.S. Bureau of Mines
Spokane Research Center
E. 315 Montgomery Ave.
Spokane, WA 99207
LIBRARY

Mission: As the Nation's principal conservation agency, the Department of the Interior has responsibility for most of our nationally-owned public lands and natural and cultural resources. This includes fostering wise use of our land and water resources, protecting our fish and wildlife, preserving the environmental and cultural values of our national parks and historical places, and providing for the enjoyment of life through outdoor recreation. The Department assesses our energy and mineral resources and works to assure that their development is in the best interests of all our people. The Department also promotes the goals of the Take Pride in America campaign by encouraging stewardship and citizen responsibility for the public lands and promoting citizen participation in their care. The Department also has a major responsibility for American Indian reservation communities and for people who live in Island Territories under U.S. Administration.

Report of Investigations 9247

Effects of Abandoned Multiple Seam Workings on a Longwall in Virginia

By Gregory J. Chekan, Rudy J. Matetic,
and David L. Dwyer

UNITED STATES DEPARTMENT OF THE INTERIOR
Manuel Lujan, Jr., Secretary

BUREAU OF MINES
T S Ary, Director

Library of Congress Cataloging in Publication Data:

Chekan, G. J. (Gregory J.)
Effects of abandoned multiple seam workings on a longwall in Virginia / by Gregory J. Chekan, Rudy J. Matetic, and David L. Dwyer.

(Bureau of Mines report of investigations; 9247)

Bibliography: p. 14

Supt. of Docs. no.: I 28.23:9247.

1. Mine subsidences–Virginia–Dickenson County. 2. Longwall mining–Virginia–Dickenson County. I. Matetic, Rudy J. II. Dwyer, David L. III. Title. IV. Series: Report of investigations (United States. Bureau of Mines); 9247.

TN23.U43 [TN319] 622 s--dc19 [622'.334'09755745] 89-600037

CONTENTS

ILLUSTRATIONS

TABLES

UNIT OF MEASURE ABBREVIATIONS USED IN THIS REPORT

ft	foot	lb/ft^3	pound per cubic foot
ft^2	square foot	pct	percent
in	inch	psi	pound per square inch
lb/ft	pound per foot	psig	pound per square inch, gauge

EFFECTS OF ABANDONED MULTIPLE SEAM WORKINGS ON A LONGWALL IN VIRGINIA

By Gregory J. Chekan,[1] Rudy J. Matetic,[1] and David L. Dwyer[2]

ABSTRACT

In order to reduce waste and improve resource conservation, mine planning, and development, the U.S. Bureau of Mines is investigating multiple seam interactions associated with longwall mining. Longwall gate entry and panel stability have been influenced by previous mining in coalbeds above and below a mine in Virginia that operates in the Lower Banner Coalbed. Directly superjacent, approximately 115 ft, the Upper Banner Coalbed has been partially worked by room-and-pillar mining. Directly subjacent, approximately 730 ft, the Tiller Coalbed has been worked by partial room-and-pillar retreat mining. The study mine has experienced problems during development of gate entries in areas of overmining and undermining. It is anticipated that stress fields associated with adjacent mining may further affect gate entry stability and face advancement during the extraction of the longwall panel.

To assess overmining and undermining effects on ground stability, the Bureau gathered geotechnical information at the site. Headgate entries and pillars were instrumented and monitored to study loading behavior as the longwall face approached and passed potential problem areas. Measurements indicate that although increases in average pillar pressure were greater than predicted values, previous mining in adjacent coalbeds had little effect on headgate stability.

[1]Mining engineer.
[2]Engineering technician.
Pittsburgh Research Center, U.S. Bureau of Mines, Pittsburgh, PA.

INTRODUCTION

In the Eastern Coal Region, over 70 billion tons of minable reserves lie in a multiple seam configuration (*1*).[3] Historically, room-and-pillar mining has dominated eastern coal production. Coalbeds were mined in no particular order, as seam sequencing was based primarily on ownership, availability, and economics, with little concern for the conservation of adjacent coals. Longwall mining technology has increased coal production, but the stress fields and fracturing induced by workings in other vertically adjacent seams can slow gate road development and longwall production, increasing the risk of mining.

Interactions between adjacent coalbeds due to undermining and overmining are documented in various case and model studies (*2-13*). Undermining results in the subsidence of overlying coalbeds and is most damaging when panel width is subcritical to critical. The magnitude and extent of damage depend upon the height of the fractured zone, which is defined by the angle of draw and the geologic and physical properties of the strata. Depending on the uniformity of extraction, empirical studies (*7-8*) approximate the fracture zone to range between 30 and 50 times the mining height. Coalbeds within 10 to 15 times the mining height may suffer severe damage. Beyond this range, the strata tend to remain intact and sag uniformly, resulting in a relatively destressed area at the point of maximum subsidence. Most ground problems in overlying coalbeds occur near the boundaries of the subsidence trough where tensile and compressive stresses form because of strata flexure. As mining develops through this trough, these stresses can cause instability in the mine structure, particularly the roof (*2-4, 10-12*).

Overmining may result in the transfer of load to pillars and entries in underlying operations. This interaction has been documented in workings separated by hundreds of feet (*2-5*), but occurs particularly when the overburden-to-innerburden ratio exceeds 10:1 and the innerburden is of a shale composition and less than 110 ft thick (*5*). Problem areas are usually located subjacent to pillar and/or gob lines or large isolated barriers in the upper seam. The stress fields induced in these areas concentrate in the innerburden and, depending on their magnitude, may cause instability in one or both operations.

The production potential of longwalls makes this mining method very economically attractive. As the number of longwall operations increases, the likelihood of encountering subjacent and superjacent workings will increase as well. Few attempts have been made in the field to document the effects of overmining and undermining on longwall development. To conserve national resources, the Bureau conducted this research to gain insight into the effects of multiple-seam workings on longwall operations. Eventually, this knowledge will lead to improvements in longwall planning, design, and production.

MINE LOCATION AND GEOLOGY

The study mine is located in Dickenson County, VA, as shown in figure 1, and is operating in the Lower Banner Coalbed. Directly superjacent, 115 ft, and subjacent, 730 ft, the Upper Banner and Tiller Coalbeds have been worked using partial room-and-pillar retreat mining. A generalized stratigraphic column of the study area is shown in figure 2. Figure 3 shows an overburden isopach map above the study longwall panel, which is the second panel to be extracted at this mine. Overburden above the headgate entry ranges from 480 to 740 ft and consists predominately of interbedded shales and sandstones. The innerburden between the Upper and Lower Banner Coalbeds consists predominantly of gray shales. The innerburden between the Tiller and Lower Banner Coalbeds consists of interbedded shales and sandstones. Other site-specific information is given in table 1.

[3]Italic numbers in parentheses refer to items in the list of references preceding the appendix at the end of this report.

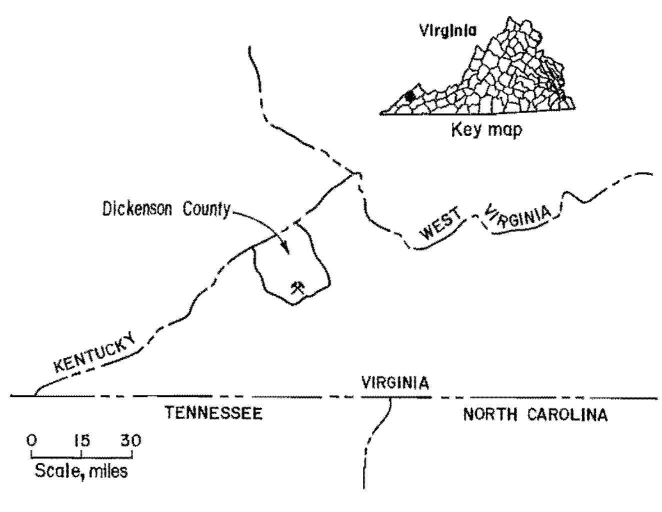

Figure 1.–Location of study mine.

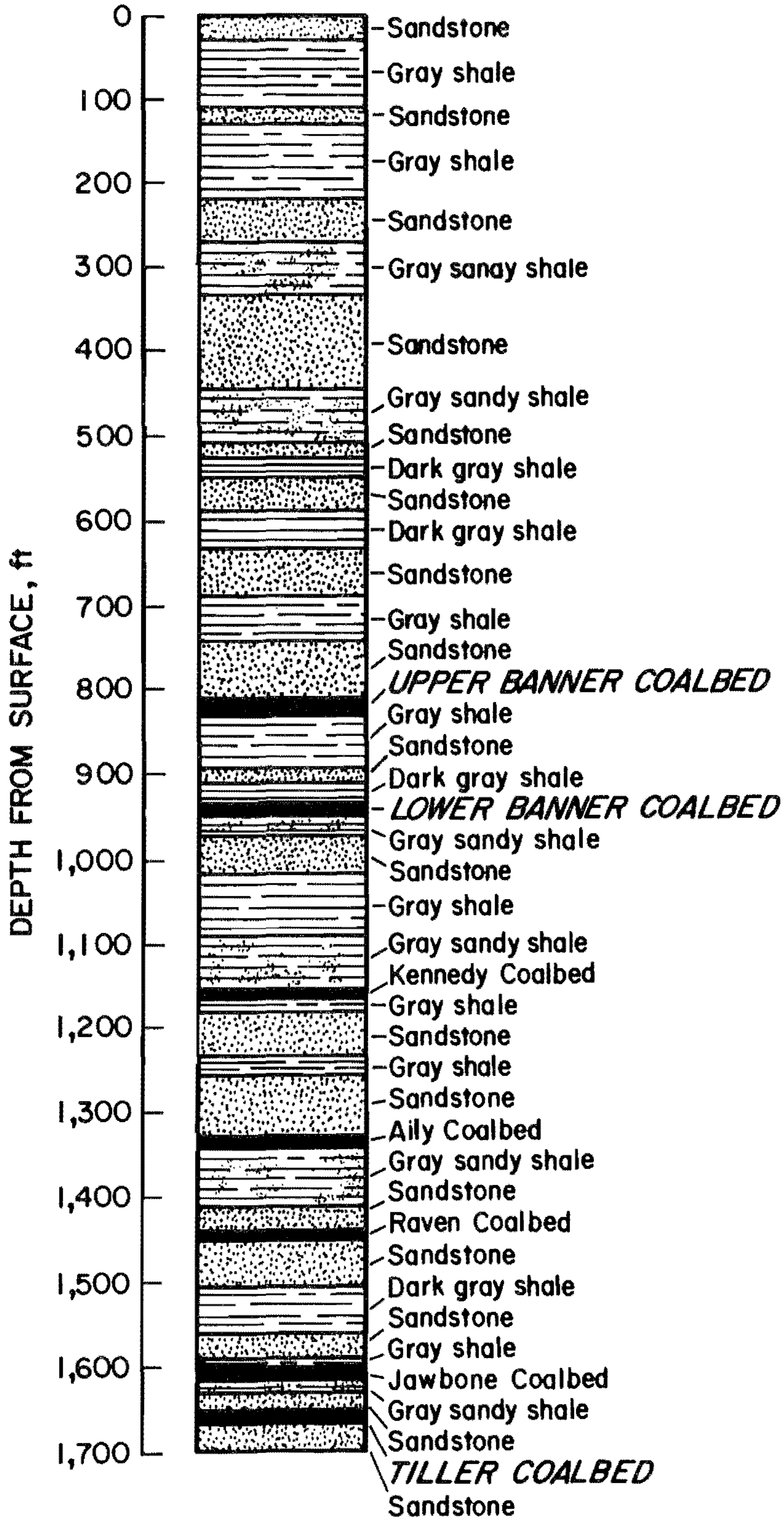

Figure 2.–Generalized stratigraphic column.

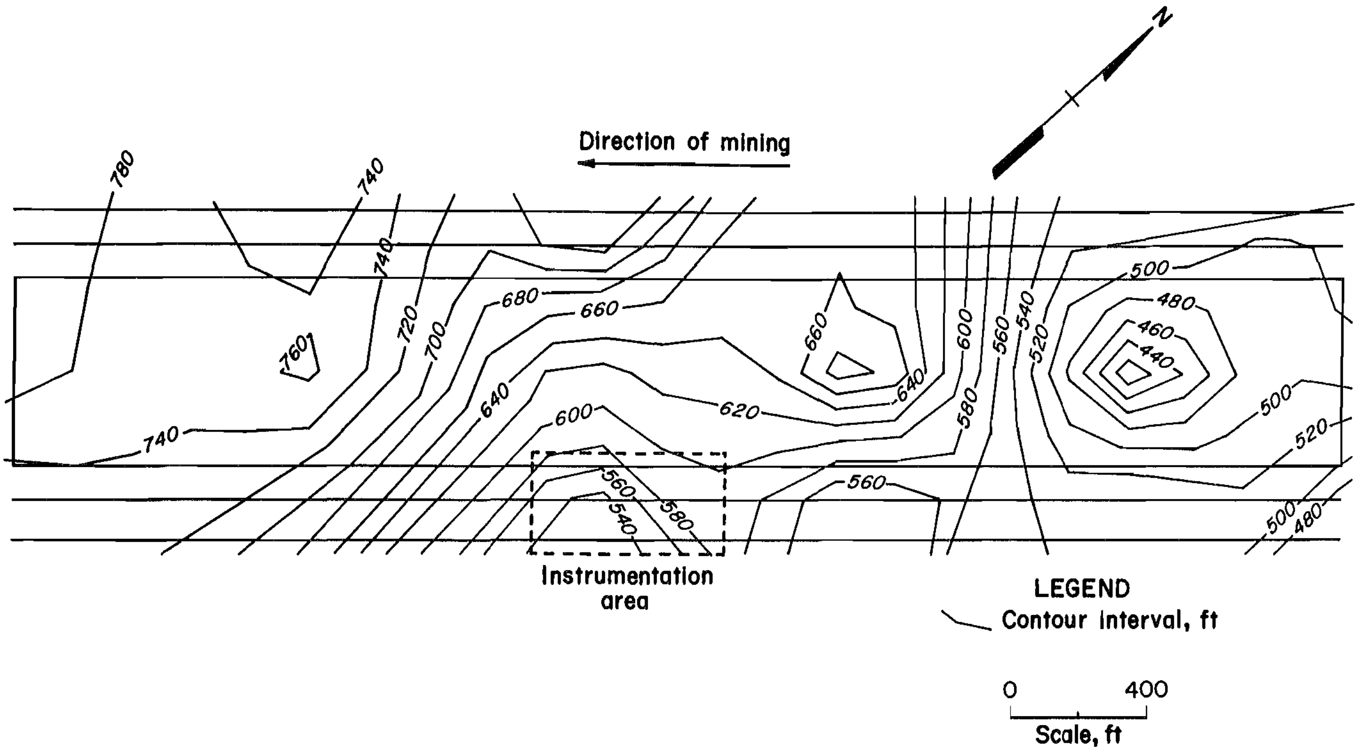

Figure 3.–Overburden above longwall panel showing instrumented area.

Table 1.–Site-specific coalbed information

	Tiller	Lower Banner	Upper Banner
Mining status	Nonactive[1]	Active	Nonactive[2]
Mining method	RP	LW	RP
Av mining height . . . in	63	46-48	80
Av entry width . . . ft	20	20	20-22
Av pillar dimension . . . ft	60 by 60	60 by 80	40 by 80
Longwall panel width . . . ft	NAp	550	NAp
Longwall panel length . . . ft	NAp	3,960	NAp
Coal characteristics, psi:			
Cubical specimen strength (σ_c)[3]	NAp	3,880	NAp
In situ coal strength (σ_c)[3]	NAp	915	NAp

LW Longwall.
NAp Not applicable.
RP Room and pillar.

[1]Closed in 1970.
[2]Closed in 1948.
[3]See appendix.

LOCATION OF INSTRUMENTATION

The area selected for instrumentation along the headgate entry is shown in figure 3. Overburden in this area ranges from 540 to 580 ft. Figures 4 and 5, respectively, show the overmining in the Upper Banner Coalbed and undermining in the Tiller Coalbed superimposed on the longwall panel. The instrumentation is located in an area where overmining and undermining leave "transition zones," which are the dividing lines between support pillars and gob. It was anticipated that the stress fields associated with these zones would complicate the longwall front and side abutments, increasing the average load on the headgate pillars.

Two types of instruments were installed in this area of the headgate–convergence stations and borehole platened flatjacks (*14*). Convergence stations were used to measure entry convergence and consist of two reference pins, one in the roof and one in the floor, between which measurements are made with a tube extensometer. Twenty-three stations were installed in the headgate and their locations are shown in figure 6.

Borehole platened flatjacks or BPF's are used to measure increases and decreases in pillar pressure. The BPF is a simple and inexpensive instrument consisting of a copper flatjack positioned between two aluminum platens. The device is installed in a 2-in-diameter borehole in the pillar, and the flatjack is inflated with hydraulic oil to a predetermined setting pressure. The BPF can be oriented in the borehole to measure pressure change in any direction. Figure 7 shows a schematic of the BPF installed in a coal pillar. Thirty-six BPF's were installed in six selected pillars as shown in figure 8. Six BPF's were installed across the half width of each pillar at depths ranging from 5 to 30 ft in 5-ft spacings. All BPF's were oriented to measure vertical changes in pillar pressure.

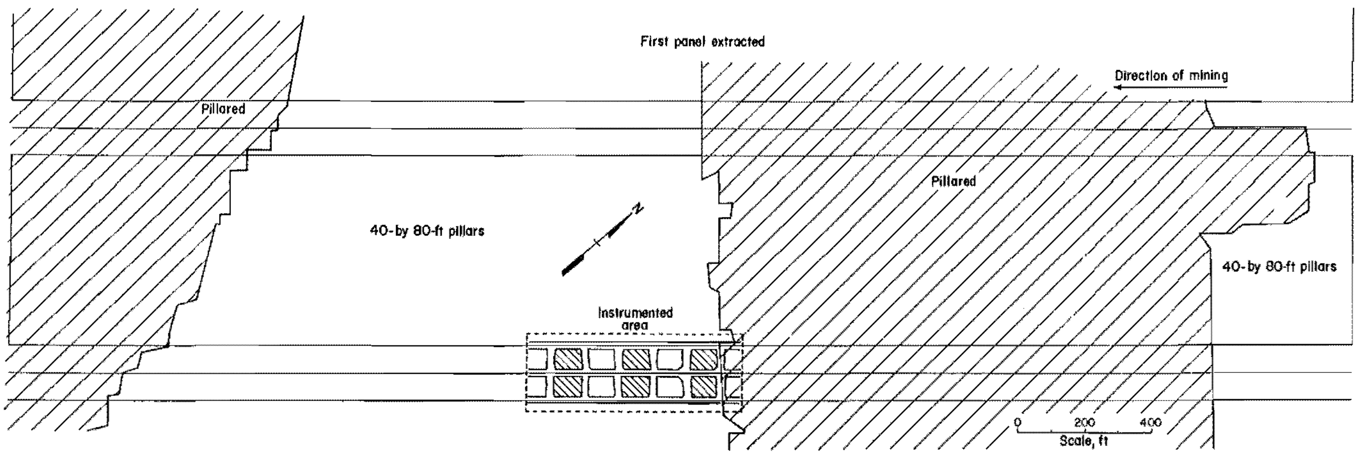

Figure 4.–Overlay of Upper Banner room-and-pillar workings on Lower Banner longwall panel.

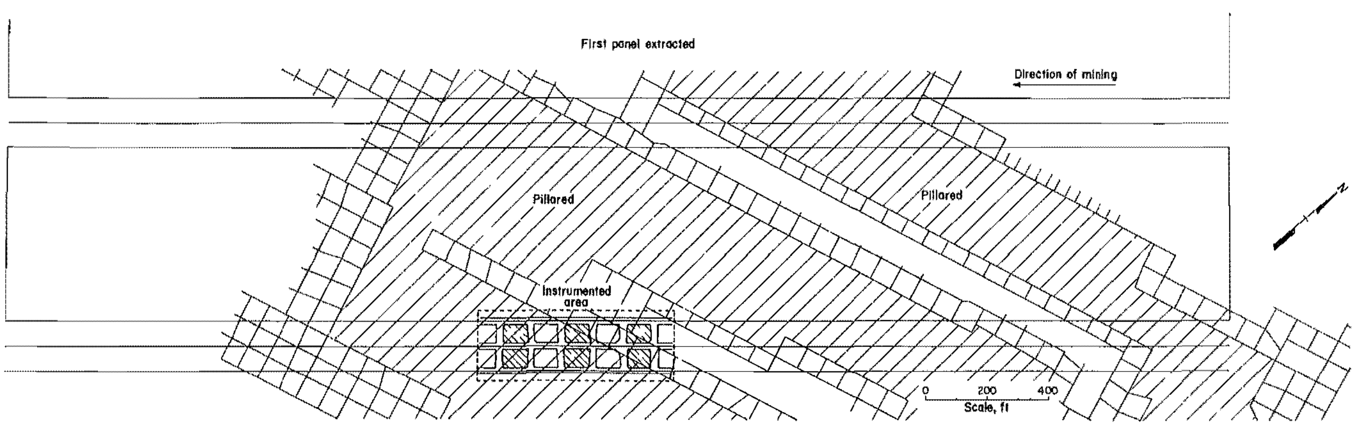

Figure 5.–Overlay of Tiller room-and-pillar workings on Lower Banner longwall panel.

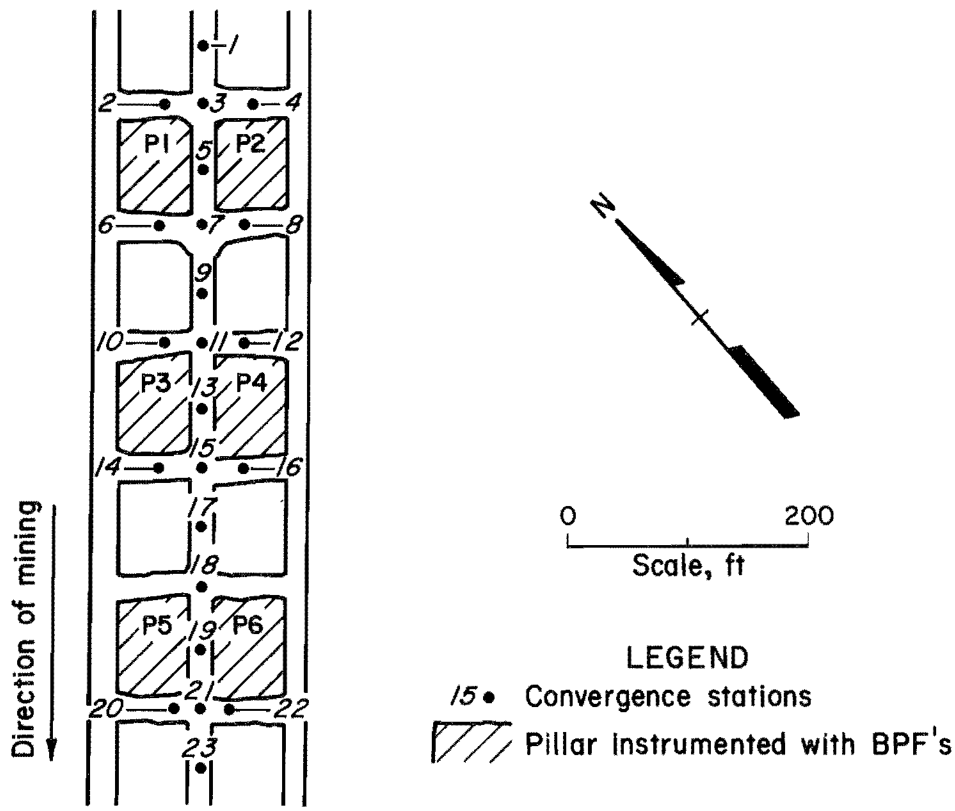

Figure 6.–Location of convergence stations in instrumented area.

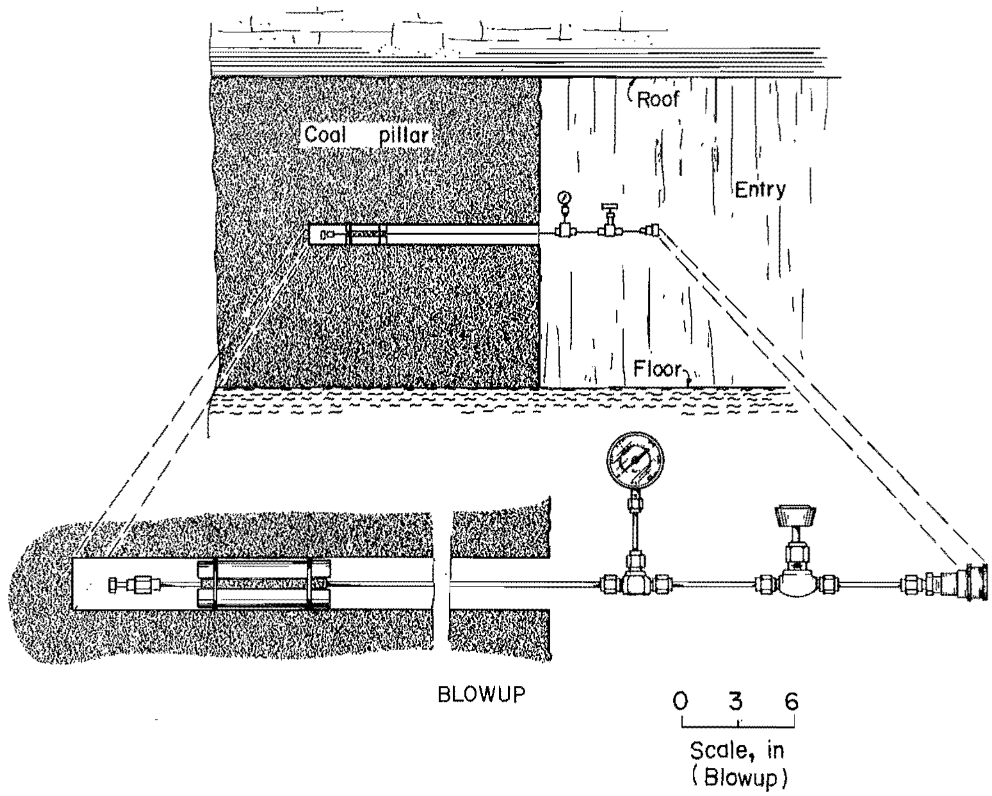

Figure 7.–Schematic of BPF installed in coal pillar.

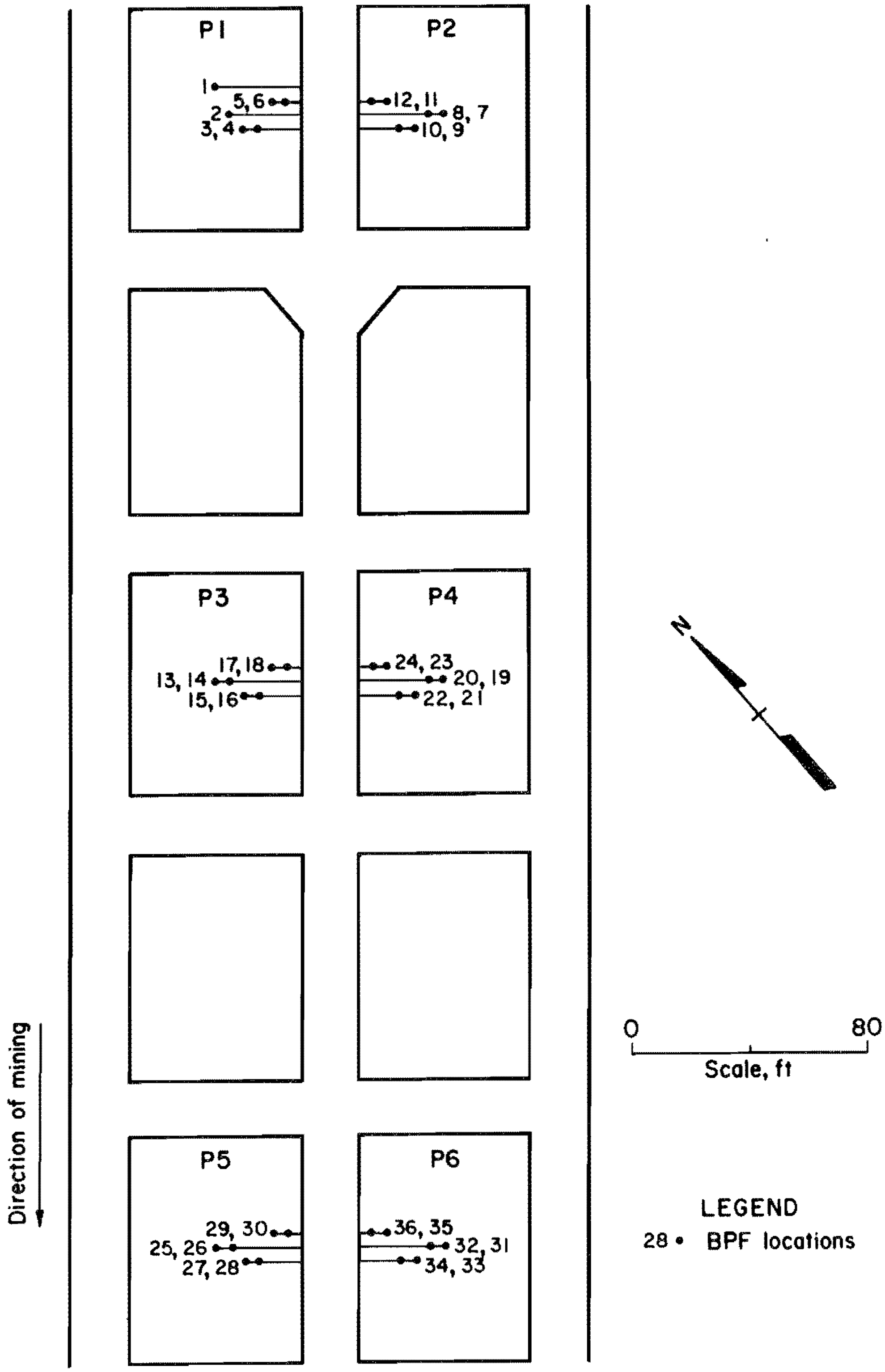

Figure 8.–Location of BPF's in six selected pillars.

RESULTS

As shown in figures 4 and 5, room-and-pillar mining in both the Upper Banner and Tiller Coalbeds was extensive, with limited areas along the headgate and panel that were not influenced by mining either above or below. The headgate and panel were 85 pct undermined as workings extended almost the entire length of the panel except for the last 450 ft. Overmining extended over the entire headgate and panel with about 45 pct of the coal left in 40- by 80-ft pillars. Therefore, since a control area of noninterference could not be established for instrumentation, a comparative analysis of measured headgate loadings could not be conducted. Instead, instruments were positioned in potential problem zones to assess measured headgate loads versus predicted values.

PREDICTING HEADGATE PILLAR LOAD

Gate entry pillars experience three separate sets of loading during their lifetime. The first loading occurs during headgate development and is a result of the weight of the overburden supported by the pillar. A second headgate loading results from the front and side abutment as the longwall approaches and passes the pillar. A third loading results in the tailgate during the extraction of a second, adjacent panel. One method for estimating the first and second headgate load is based on the tributary area method (TAM) and the concept of the abutment angle (*15*). The development load per unit length of gate entry is represented by the following equation:

$$L_t = H\,[W_{pt} + (n\text{-}1)W_e]\gamma, \tag{1}$$

where L_t = development load per unit length of entry, lb/ft,

H = depth of cover, ft,

W_{pt} = the total width of the pillars across the gate entries, ft,

n = the number of gate entries,

W_e = gate entry width, ft,

and γ = average unit weight of overburden, 160 lb/ft^3.

The side abutment is defined as the additional load supported by the pillar after the face has passed. The load per unit length of gate entry is represented by the following equation:

$$L_s = H\,(\tan\beta)\gamma/2, \tag{2}$$

where L_s = side abutment load per unit length of gate entry, lb/ft,

H = depth of cover, ft,

β = the abutment angle, 21° (*15*),

and γ = average unit weight of overburden, 160 lb/ft^3.

The front abutment is defined as the average load increase experienced by the pillar when the longwall face is parallel to that pillar. It is represented by the following equation:

$$L_f = (F)(L_s), \tag{3}$$

where L_f = front abutment load per unit length of gate entry, lb/ft,

F = front abutment factor, 0.51 (*15*),

and L_s = side abutment load per unit length of gate entry, lb/ft.

To convert these linear loads (L_t, L_s, L_f) from pound per foot to a load per unit area, pound per square inch, the following equation is used:

$$\sigma_t, \sigma_f, \sigma_s = (L_t, L_f, L_s)\,C/144\,A_{pt}, \tag{4}$$

where σ_t = average stress on pillar after development, psi,

σ_f = average increase in pillar stress due to the front abutment, psi,

σ_s = average increase in pillar stress due to the side abutment, psi,

L_t = overburden load, lb/ft,

L_s = side abutment load, lb/ft,

L_f = front abutment load, lb/ft,

C = crosscut spacing, ft,

and A_{pt} = the total area of the pillars, ft^2.

Table 2 lists the values for σ_s and σ_f, in the instrumented area of the headgate, and the values of other variables in equations 1, 2, 3, and 4. The σ_s and σ_f values do not take into account the development stress (σ_t), supported by the pillar, and therefore represent additional loads.

Table 2.–Predicted longwall abutment stresses in study area

Depth of cover (H)	ft	570
Number of gate entries (n)		3
Total width of pillars across gate entries (W_{pt})	ft	120
Gate entry width (W_e)	ft	20
Crosscut spacing (C)	ft	100
Total area of pillars (A_{pt})	ft^2	9,600
Overburden load (L_t)	10^7 lb/ft	1.46
Side abutment load (L_s)	10^6 lb/ft	9.97
Front abutment load (L_f)	10^6 lb/ft	5.08
Av stress on pillar after development (σ_t)	psi	1,060
Av increase in pillar stress--		
From side abutment load (σ_s)	psi	720
From front abutment load (σ_f)	psi	370

CONVERGENCE STATIONS

To assess the effects of subsidence, caused by undermining, on headgate stability in the transition area, convergence stations were utilized. Case study and model analysis (*7-8, 12*) have shown that undermining usually results in poor roof conditions in the upper workings. Empirical studies (*7-8*) estimate the subsidence fracture zone to range between 30 to 50 times the mining height. Coalbeds within this range may experience some interaction, increasing the risk and cost of development. In this case, the active workings lie well beyond this range as the Tiller Coalbed is approximately 63 in thick with 730 ft of innerburden to the Lower Banner Coalbed. The headgate experiences minimal roof problems during development and generally remained in good condition until approach of the longwall face.

Convergence measurements were initiated when the longwall face was 400 ft approaching station 1. Figures 9, 10, and 11 graph cumulative convergence versus longwall face position for selected stations across the width of the headgate. The graphs show that convergence rates increased once the face passed a particular station (denoted by longwall face position of 0 ft). The observation is especially evident for stations 6, 10, and 14 located in crosscuts closest to the panel. Roof conditions slowly deteriorated as the longwall face advanced but remained in good condition until the face was over 1,000 ft past the instrumented area.

Table 3 lists the final convergence readings after which roof conditions were considered too poor to continue monitoring. Figure 12 plots the convergence contours based on these final readings. These contours show convergence to be maximum in entries closest to the longwall panel but gradually decreasing across the headgate width. Both the

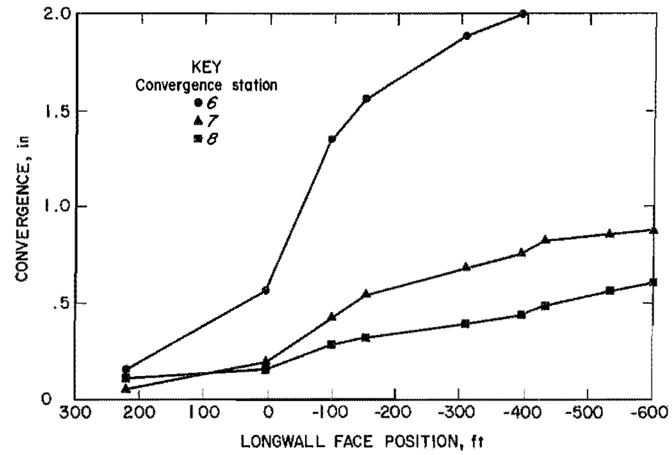

Figure 9.–Cumulative convergence versus longwall face position for stations 6, 7, and 8.

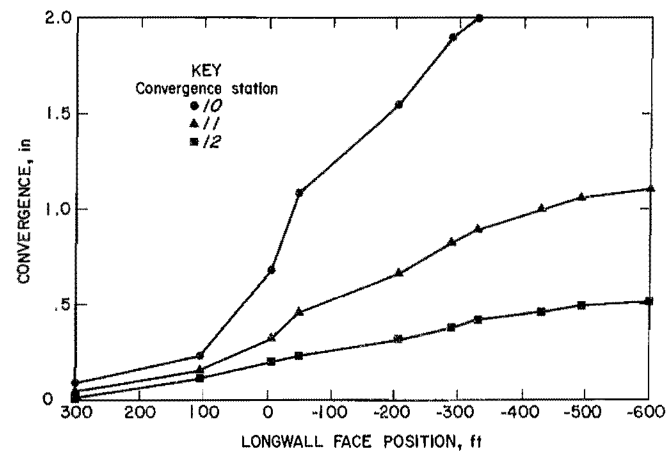

Figure 10.–Cumulative convergence versus longwall face position for stations 10, 11, and 12.

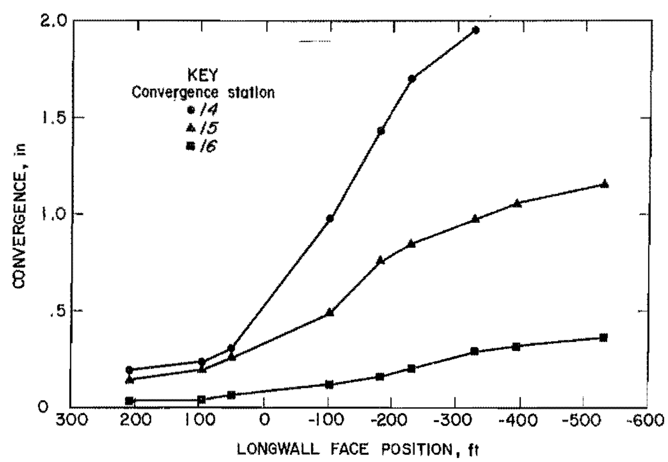

Figure 11.–Cumulative convergence versus longwall face position for stations 14, 15, and 16.

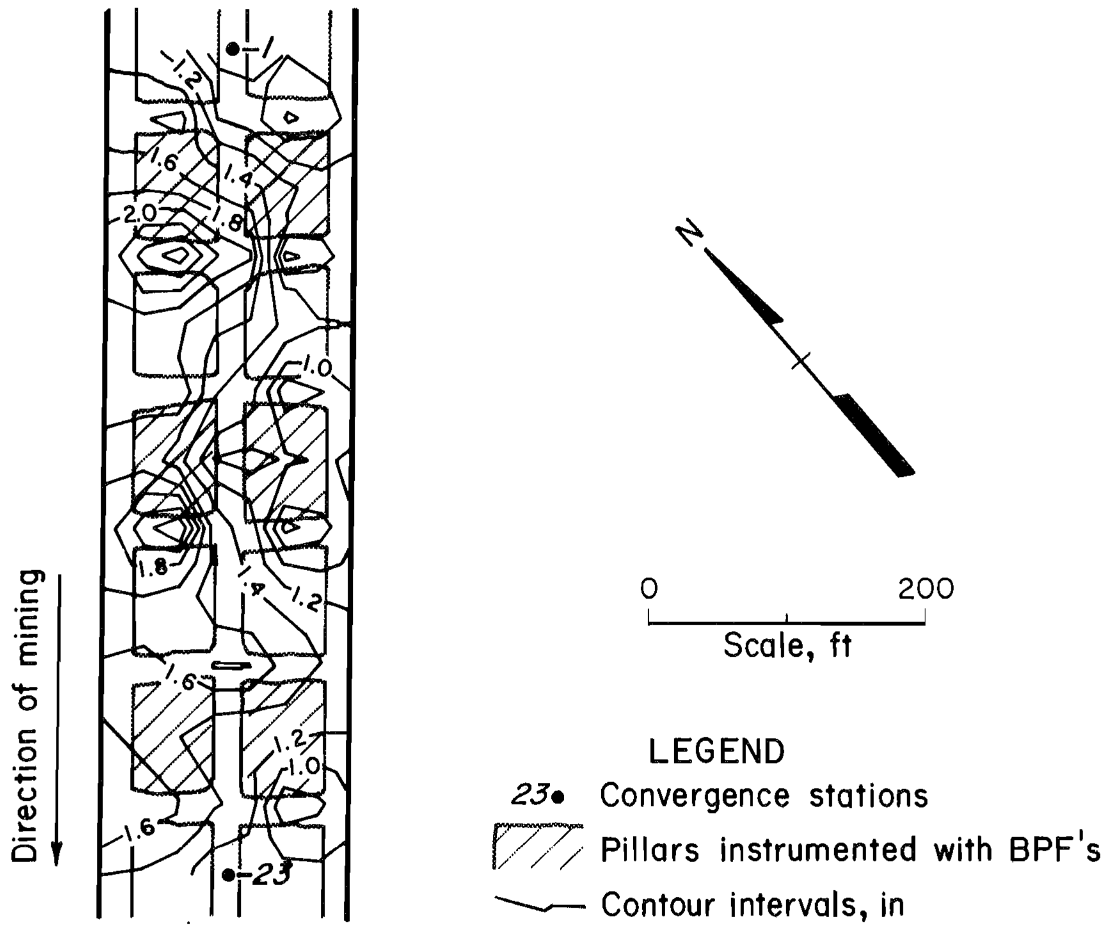

Figure 12.–Convergence contours based on final convergence measurements.

Table 3.–Final convergence for stations 1 through 23

Convergence station	Longwall face position past station, ft	Final convergence, in
1	1,600	0.522
2	1,540	1.712
3	1,540	.829
4	1,540	.519
5	1,500	1.511
6	1,440	2.807
7	1,440	2.358
8	1,440	.649
9	1,400	1.604
10	1,340	2.063
11	1,340	1.342
12	1,340	.593
13	1,300	.785
14	1,240	2.175
15	1,240	1.389
16	1,240	.470
17	1,200	1.477
18	1,140	1.921
19	1,100	1.179
20	1,040	1.734
21	1,040	1.456
22	1,040	.572
23	1,000	.980

immediate roof and floor were composed of a black, fine-grain shale several feet thick, overlain and underlain by thicker, more competent sandstone units. Although no instruments were used to differentiate between roof sag and floor heave, it appeared that most convergence was a result of roof sag. The floor remained intact and in good condition well after passage of the longwall face, but the roof was highly fractured with the immediate shale top falling in many areas.

Underground observation also noted that in subsided areas the front abutment would fracture the headgate roof 20 to 30 ft in advance of the longwall face. This fracturing required the installation of supplemental supports (timbers, cribs, etc.), especially at intersections, to maintain stability. In the last 450 ft of the headgate, where no lower seam mining had taken place, the front abutment had a less severe effect on the roof and additional supports were not required.

BOREHOLE PLATENED FLATJACKS

BPF's were installed to determine if overmining would affect the loading behavior of the headgate pillars during longwall panel extraction. Interactions between operations, as a result of pillar load transfer, are more likely to occur when innerburden is less than 110 ft and overburden-to-innerburden ratio is 10:1 or greater. At this site, innerburden is 115 ft and overburden-to-innerburden ratio is 5:1.

BPF readings were initiated when the longwall face was approximately 400 ft away and approaching pillars P1 and P2 and continued until the face was over 1,000 ft past pillars P5 and P6. Setting pressure for all 36 BPF's was 1,000 psig. Calibration tests conducted on BPF's suggest that at this setting pressure, the change in BPF gauge pressure as it relates to changes in strata pressure is a 1:1 ratio (*14*). Figures 13 and 14 graph the recorded pressure changes for BPF's 1 through 5, 7, and 9 through 12, as the longwall face approached and passed the first set of instrumented pillars, P1 and P2. The pressure changes shown in these graphs are similar in trend to the pressure changes that occurred in the other four instrumented pillars. Typically, pressure increases were first detected when the longwall face was 200 ft away and approaching the instrumented pillar. Pressure continued to increase until the longwall face was 400 to 500 ft past the pillar, then gradually stabilized.

Table 4 lists the final pressure increase readings for the 36 BPF's and the average pressure increase experienced by each pillar due to the side abutment. These increases represent pressure changes over the initial setting pressure of 1,000 psig. Figures 15, 16, and 17 graph these final pressure increases versus the BPF position across the headgate width.

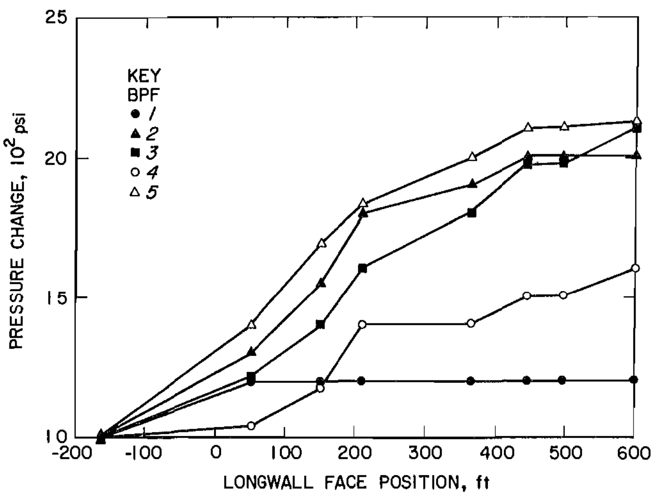

Figure 13.–BPF pressure increase versus face position for pillar P1.

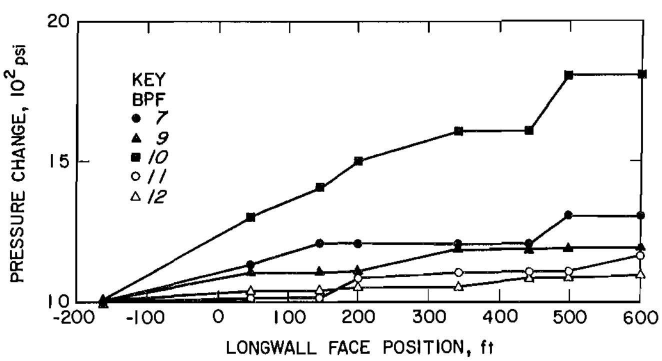

Figure 14.–BPF pressure increase versus face position for pillar P2.

Table 4.–Final pressure increases for BPF's 1 through 36

(BPF setting pressure, 1,000 psig)

Pillar and BPF	Installation depth, ft	Longwall face position past BPF, ft	Pressure, psi: Increase	Pressure, psi: Av per pillar[2]
P1:				
1 . . .	30	1,500	200	900
2 . . .	25		1,000	
3 . . .	20		1,600	
4 . . .	15		500	
5 . . .	10		1,200	
6 . . .	5		(1)	
P2:				
7 . . .	30	1,500	300	380
8 . . .	25		(1)	
9 . . .	20		200	
10 . .	15		900	
11 . .	10		300	
12 . .	5		200	
P3:				
13 . .	30	1,300	1,600	1,400
14 . .	25		1,400	
15 . .	20		1,200	
16 . .	15		1,400	
17 . .	10		1,400	
18 . .	5		(1)	
P4:				
19 . .	30	1,300	500	575
20 . .	25		200	
21 . .	20		(1)	
22 . .	15		(1)	
23 . .	10		600	
24 . .	5		1,000	
P5:				
25 . .	30	1,100	2,000	1,480
26 . .	25		3,000	
27 . .	20		1,000	
28 . .	15		300	
29 . .	10		1,000	
30 . .	5		1,600	
P6:				
31 . .	30	1,100	400	435
32 . .	25		400	
33 . .	20		200	
34 . .	15		500	
35 . .	10		400	
36 . .	5		700	

[1]BPF inoperable.
[2]Overall average for the 31 operable BPF's is 875 psi.

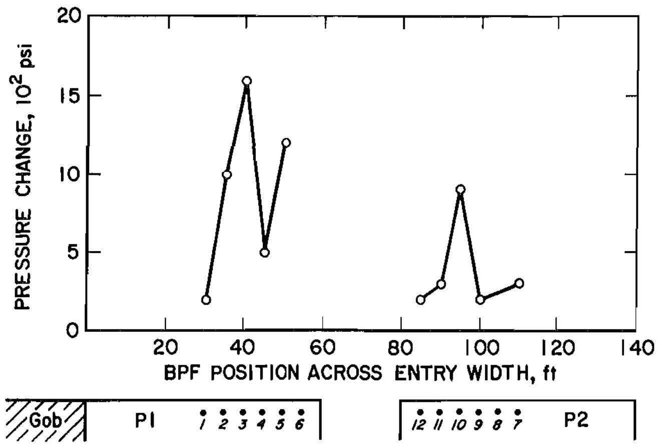

Figure 15.–Loading profile across headgate width due to side abutment load for pillars P1 and P2.

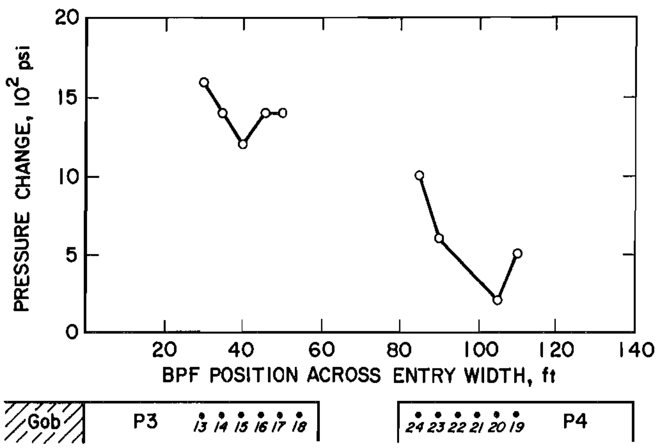

Figure 16.–Loading profile across headgate width due to side abutment load for pillars P3 and P4.

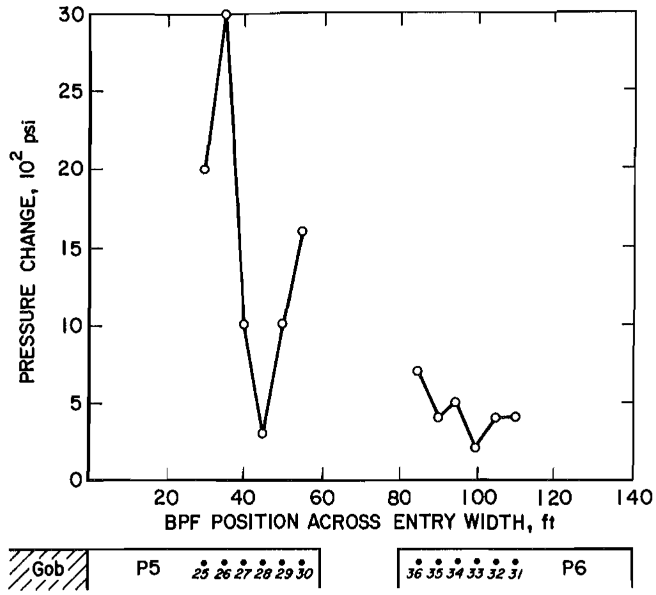

Figure 17.–Loading profile across headgate width due to side abutment load for pillars P5 and P6.

The profiles in figures 15 through 17 show that pillars closest to the longwall panel, P1, P3, and P5, absorbed most of the side abutment load. The average pressure increase in each of these three pillars, as shown in table 4, was greater than the predicted value of 720 psi. The loading profiles also show that pillar pressure gradually decreased across the headgate width. The average pressure increase (table 4) for pillars P2, P4, and P6, located furthest from the longwall panel, were less than the predicted side abutment value. For the entire BPF array, the average side abutment load experienced by all six pillars was 875 psi. This value is slightly greater than the predicted side abutment load of 720 psi.

Research conducted at single seam longwall sites (*16*) has shown that stress across the pillar width is not always symmetric, but can be higher, specifically on the pillar side closest to the longwall panel. Because the pillars of this study were instrumented across their half width, the side abutment load may be greater than recorded values.

PILLAR SAFETY FACTORS

Additional loads imposed on pillars resulting from multiple seam mining and during longwall panel extraction can cause instability in the gate entries. This is particularly true if pillars are not properly designed with adequate safety factors to contend with this load transfer. There are many methods available for calculating pillar strength and resulting safety factors. Research has shown (*17*) that pillar strength is characterized by two effects: the shape effect and the size effect. The more commonly used pillar design formulas take these two factors into consideration. These methods account for the differences in the strength reduction between small size specimens tested in the laboratory and full size coal pillars mined in situ. From available pillar design methods the following four formulas are most applicable to room-and-pillar coal mines.

Obert-Duvall–

$$\sigma_p = \sigma_1 \ (0.778 + 0.222 \ w/h), \tag{5}$$

Holland-Bureau–

$$\sigma_p = \sigma_1 \ (w/h)^{1/2}, \tag{6}$$

Holland-Gaddy–

$$\sigma_p = \sigma_{c/h} (Dw)^{1/2}, \qquad (7)$$

Bieniawski-Pennsylvania State University–

$$\sigma_p = \sigma_1 (0.64 + 0.36 \, w/h), \qquad (8)$$

where σ_p = strength of mine pillar, psi,

σ_c = cubical specimen strength, psi,

σ_1 = in situ coal strength, psi (see appendix),

D = side dimension of cubical specimen, in,

h = height of pillar, in,

and w = least width of pillar, in.

These formulas can be used in conjunction with σ_t from equation 4 (which assumes the pillar to be gravity loaded only) to determine the pillar safety factors.

Table 5 lists the safety factors for pillars P2 and P5, the lower and upper limit of measured pillar load (see table 4). Safety factors after development are calculated by dividing the pillar strength (σ_p) by the development load (σ_t). Safety factors after side abutment loading are calculated by dividing pillar strength (σ_p) by the measured load on pillar after side abutment loading.

Pillar strength and safety factors for this analysis were derived by using the ultimate strength approach. This design method makes two assumptions: (1) pillar strength is related to the uniform, ultimate strength derived by scaling uniaxial strength values from laboratory specimens; and (2) an average pillar stress or load exists across the pillar in situ. Recommended safety factors for pillars designed by this approach generally range between 1.5 and 2.2 (*17*). Safety factors after development met this condition as values ranged from 2.8 to 5.2 for all four methods. For pillar P2, the lower limit of measured pillar load, the safety factors remained above 2.0 after side abutment loading. For pillar P5, the upper limit of measured pillar load, safety factors as calculated by all four methods remained above 1.0.

Field studies that relate pillar stability to depth and innerburden thickness suggest that when overburden-to-innerburden ratios exceed 10:1, the workings may be unstable. Site-specific variations in geology and mine geometry will influence this ratio, but for the most part, case study documentation validates this trend, particularly when innerburden is less than 110 ft. Under these conditions, pillars designed with lower limit safety factors (1.5 or less) may experience instability because of stresses produced by mining in adjacent seams.

For this study, overburden-to-innerburden ratio was 5:1 and innerburden thickness was 115 ft. Safety factors for headgate pillars after development were within the recommended range in the study area. Observations on ground conditions showed that the pillars experienced some slight rib spalling after side abutment loading, but remained intact and very stable even though longwall side abutment loads reduced the safety factors to near 1.

Table 5.–Safety factors for pillars P2 and P5

	P2	P5
Development load (σ_t) . . . . psi . .	1,060	1,060
Average increase in pillar pressure due to side abutment . . . . psi . .	380	1,480
Estimated load on pillar after side abutment . . . . psi . .	1,440	2,540
Pillar strength (σ_p), psi (*17*):		
Obert-Duvall	3,760	3,760
Holland-Bureau	3,540	3,540
Holland-Gaddy	3,070	3,070
Bieniawski-Pennsylvania State Univ.	5,530	5,530
Safety factor after development (*17*):		
Obert-Duvall	3.5	3.5
Holland-Bureau	3.3	3.3
Holland-Gaddy	2.8	2.8
Bieniawski-Pennsylvania State Univ.	5.2	5.2
Safety factor after side abutment loading (*17*):		
Obert-Duvall	2.6	1.5
Holland-Bureau	2.4	1.4
Holland-Gaddy	2.1	1.2
Bieniawski-Pennsylvania State Univ.	3.8	2.1

CONCLUSIONS

Accurate prediction of multiple seam interactions can be difficult, especially when mine layouts are as geometrically complex as in this study. Through careful premine planning and analysis, potential problem areas can be reasonably predicted and avoided if necessary. Geotechnical instrumentation for monitoring workings suspect of interaction is a feasible method for evaluating site-specific stability problems. Information such as rock strengths, entry convergence rates, and the characteristic loadings of pillars can be correlated with the geologic environment and determinations made concerning the extent and magnitude of interaction. From this information, proper roof spans, pillar safety factors, and support requirements can be established, within reason, for maintaining stability.

From the research, the following site-specific conclusions can be made.

1. Load transfer due to the transition zone in the Upper Banner Coalbed had little effect on the side abutment load as pillar were stressed slightly more than predicted values. Pillar P5 recorded the highest average increase in pressure of 1,480 psi, twice the predicted value of 720 psi, but this did not influence overall headgate stability. The average pressure increase due to the longwall side abutment for the entire instrument array was 875 psi.

2. Using the ultimate strength approach, pillar safety factors exceeded recommended values. Safety factors after development ranged between 3.5 and 5.2, well over the upper limit of 2.2. Side abutment loading lowered these values near 1, but headgate pillars satisfactorily controlled abutment loads as well as any additional loads induced by overmining.

3. Convergence measurements indicate that undermining in the Tiller Coalbed caused no appreciable damage to the Lower Banner workings. The headgate experienced minimal roof problems during development and remained in good condition until approach of the longwall face. Underground observation noted that in undermined areas, the front abutment would fracture the headgate roof 20 to 30 ft in advance of the face, which required the installation of supplemental support to maintain headgate stability. In the last 450 ft of the headgate, where no undermining had taken place, roof fracturing due to front abutment loading was not apparent and supplemental supports were not required.

REFERENCES

1. Singh, M. A., and M. F. Dunn. Investigation of Problems and Benefits of Underground Multiple Seam Mining (U.S. Dep. Energy contract DEAC01-79ET14242, Eng. Int., Inc.). DOE/FE/3218-1, Aug. 1981, 292 pp.

2. Stemple, D. T. A Study of Problems Encountered in Multiple Seam Coal Mining in the Eastern U.S. Bull. VA Polytech. Inst., v. 49, No. 5, Mar. 1956, 65 pp.

3. Dunham, R. K., and R. L. Stace. Interaction Problems in Multi-Seam Mining. Paper in Proceedings of the 19th Symposium on Rock Mechanics (Proc. Conf. McKay Sch. Mines, Stateline, NV, May 1-2, 1978). Univ. NV, Reno, NV, 1978, pp. 174-179.

4. King, H. J., B. N. Whittaker, and A. S. Batchelor. The Effects of Interactions in Mine Layouts. Paper 17 in Proceedings of the Fifth International Strata Control Conference. Natl. Coal Board, London, 1972, 11 pp.

5. Haycocks, C., B. Ehgartner, M. Karmis, and E. Topuz. Pillar Load Transfer Mechanisms in Multi-Seam Mining. Soc. Min. Eng. AIME preprint 82-69, 1982, 7 pp.

6. Haycocks, C., M. Karmis, and B. Ehgartner. Multiple Seam Mine Design. Paper in State-of-the-Art of Ground Control in Longwall Mining and Mining Subsidence. Soc. Min. Eng. AIME, 1982, pp. 59-65.

7. Haycocks, C., M. Karmis, E. Barko, J. Carman, B. Ehgartner, S. Hudock, and S. Webster. Ground Control Mechanisms in Multi-Seam Mining (grant G1115511, VA Polytech. Inst. and State Univ.). BuMines OFR 7-84, 1983, 328 pp.

8. Peng, S. S., and U. Chandra. Getting the Most From Multiple Seam Reserves. Coal Min. and Proc., v. 17, No. 11, 1980, pp. 78-84.

9. Haycocks, C., M. Karmis, and E. Topuz. Optimizing Productive Potential in Multi-Seam Underground Coal Mining. Paper in Symposium on Underground Mining (Proc. Coal Conf. and Expo VI, Louisville, KY, Oct. 27-29, 1981). McGraw-Hill, 1981, pp. 11-163.

10. Holland, C. T. Effects of Undermined Seams of Coal by Mining Seams Above or Below. Proc., WV Acad. Sci., 1947, pp. 113-132.

11. ____. Multiple Seam Mining. Coal Age, v. 56, No. 8, 1951, pp. 89-93.

12. Chekan, G. J., R. J. Matetic, and J. A. Galek. Strata Interactions in Multiple-Seam Mining–Two Case Studies in Pennsylvania. BuMines RI 9056, 1986, 17 pp.

13. Matetic, R. J., G. J. Chekan, and J. A. Galek. Pillar Load Transfer Associated With Multiple-Seam Mining. BuMines RI 9066, 1987, 23 pp.

14. Bauer, E. R., G. J. Chekan, and J. L. Hill III. A Borehole Instrument for Measuring Mining-Induced Pressure Changes in Underground Coal Mine. Paper in Research and Engineering Applications in Rock Masses, ed. by F. Ashworth (Proc. 26th U.S. Symp. on Rock Mech., SD Sch. Mines and Technol., Rapid City, SD, June 26-28, 1985). A. A. Balkema, 1985, pp. 1075-1084.

15. Mark, C., and Z. T. Bieniawski. An Empirical Method for the Design of Chain Pillars for Longwall Mining. Ch. in Rock Mechanics: Key to Energy Production, ed. by H. L. Hartman (Proc. 27th U.S. Symp. on Rock Mech., Univ. of AL, Tuscaloosa, AL, June 23-25, 1986). Soc. Min. Eng. AIME, 1986, pp. 415-423.

16. Listak, J. M., J. C. Zelanko, and T. M. Barton. Effects of Various Longwall Chain Pillar Configurations on Gate Road Stability. BuMines RI 9184, 1988, 17 pp.

17. Bieniawski, Z. T. Improved Design of Room-and-Pillar Coal Mining (U.S. Dep. Energy grant DE-FG01-78ET-11428, PA State Univ.). DOE/ET/11428T1, 1982, 165 pp.

APPENDIX.–DETERMINATION OF IN SITU COAL STRENGTH (17)[1]

Test specimens from the Lower Banner Coalbed were prepared from 2.2-in-diameter coal cores with a length-to-width ratio of 2:1. The core specimens had an average unconfined uniaxial compressive strength, σ_{spec}, of 3,180 psi.

Research has shown the correction factor from the core strength, σ_{spec}, to the strength of 2-in cubical specimen, σ_c, can be obtained through the following equation:

$$\sigma_c = \sigma_{spec} [0.778 + 0.222 (1/D)], \qquad \text{(A-1)}$$

where σ_c = uniaxial compressive strength of 2-in cube specimen, psi,

σ_{spec} = uniaxial compressive strength of core specimen, psi,

1 = length of core specimen, in,

and D = diameter of core specimen, in.

Therefore σ_c = 3,180 [0.778 + 0.222 (4.0/2.0)], or 3,880 psi.

Research has also shown that the scaling of coal properties from cubical specimens to the in situ coal strength value can be obtained through the following equation:

$$\sigma_1 = \sigma_c (D/36)^{1/2}, \qquad \text{(A-2)}$$

where σ_1 = in situ coal strength, psi,

σ_c = uniaxial compressive strength of a 2-in cube specimen, psi,

and D = cube size dimension.

Therefore $\sigma_1 = 3{,}880\ (2/36)^{1/2}$, or 915 psi.

[1]Underlined number in parentheses refers to items in the list of references preceding this appendix.